Helix versus sheet formation in a small peptide

Yong Peng and Ulrich H. E. Hansmann*
Department of Physics, Michigan Technological University, Houghton, Michigan 49931-1291, USA
(Received 12 June 2003; published 20 October 2003)

Segments with the amino acid sequence EKAYLRT (glutamine-lysine-alanine-tyrosine-leucine-arginine-threonine) appear in naturally occurring proteins both in α-helices and β-sheets. For this reason, we have used this peptide to study how secondary structure formation in proteins depends on the local environment. Our data rely on multicanonical Monte Carlo simulations where the interactions among all atoms are taken into account. Results in gas phase are compared with that in an implicit solvent. We find that both the solvated molecule and EKAYLRT in gas phase form an α-helix when not interacting with other molecules. However, in the vicinity of a β-strand, the peptide forms a β-strand. Because of this change in secondary structure our peptide may provide a simple model for the $\alpha \rightarrow \beta$ transition that is supposedly related to the outbreak of prion diseases and similar illnesses.

DOI: 10.1103/PhysRevE.68.041911 PACS number(s): 87.15.Aa, 87.15.He, 87.15.Cc

I. INTRODUCTION

Despite considerable progress over the last decade, the problem of predicting the biological active structure of a protein solely from the sequence of amino acids has remained a formidable problem. More successful have been attempts to predict only the secondary structure. Given the protein sequence it is today possible to determine the distribution and location of α-helices and β-sheets with up to 90% probability. This high success rate indicates a close relation between sequence information and secondary structure. However, two observations indicate that this relation is not a simple one. First, certain sequences can form either α-helices or β-sheets [1]. The most prominent example is the 11-residue Chameleon peptide [2] that folds as an α-helix when replacing residues 22–32 of the primary sequence of the Ig*G*-binding domain of protein *G* (57 amino acids), but as a β-strand when inserted instead of residues 42–52. Second, it has become clear over the past years that misfolding of proteins, often involving formation of β-sheets instead of α-helices, and subsequent aggregation is the cause of various illnesses including Alzheimer's disease, bovine spongiform encephalopathy, and other prion diseases. Hence, it is important to understand in detail how secondary structure formation and its role in the folding process depends on the intrinsic properties of the protein and the interaction with the surrounding environment.

In order to study these questions, we have simulated a peptide whose sequence of amino acids EKAYLRT (glutamine-lysine-alanine-tyrosine-leucine-arginine-threonine) appears in naturally occurring proteins with significant frequency at positions of both α-helices and β-sheets. Our present work differs therefore from previous investigations where we have focused on helix formation and folding in homopolymers and artificial peptides [3–8]. Unlike these molecules that have a strong intrinsic tendency to form one specific kind of secondary structure elements (α-helices), EKAYLRT allows one to research the selection of either helix or sheet, or the transition between these two secondary structures, as a function of external factors.

Our work differs from similar approaches [9,10] in that we study not minimal models but simulate detailed representations of our peptides where the interactions between all atoms are taken into account. EKAYLRT is simulated both in gas phase and with an implicit solvent. Quantities such as energy, specific heat, sheetness, and helicity are calculated as functions of temperature. We find that both the solvated molecule and EKAYLRT in gas phase form an α-helix when not interacting with other molecules. However, in the vicinity of a β-sheet the peptide prefers also to form strand. Because of the resulting ''autocatalytic'' property our peptide may therefore provide a simple model for the $\alpha \rightarrow \beta$ transition and the resulting aggregation process in some proteins that is supposedly related to the outbreak of neurological diseases such as Alzheimer's and the prion diseases.

II. METHODS

Our aim here is to research how secondary structure formation and its role in the folding process depend on either the intrinsic properties of a protein or its interaction with the surrounding environment. For this purpose, we have considered detailed, all-atom representations of peptides that are based on the sequence of amino acids EKAYLRT. To be more specific, the peptide NH_2-EKAYLRT-COOH is studied both as an isolated molecule and when interacting with another EKAYLRT peptide that is held in a β-strand conformation. Since our program package SMMP [12] in its current version allows only the simulation of single peptides we have modeled the latter case by considering the peptide NH_2-EKAYLRT-GGGG-EKAYLRT-COOH, with the *C*-terminal EKAYLRT residues kept as a β-strand. The four glycine residues form a flexible chain that holds the two peptides together but allows their relative positions to vary. The underlying assumption is that the interaction between the two EKAYLRT chains is the dominant term and their interaction with the glycine residues can be neglected.

The intramolecular interactions are described by a standard force field, ECEPP/3 [11] (as implemented in the pro-

*Corresponding author. Email address: hansmann@mtu.edu

gram package SMMP [12]) and are given by

$$E_{\mathrm{ECEPP/3}}=E_C+E_{vdW}+E_{HB}+E_{tor}, \tag{1}$$

$$E_C=\sum_{(i,j)}\frac{332q_iq_j}{\epsilon r_{ij}}, \tag{2}$$

$$E_{vdW}=\sum_{(i,j)}\left(\frac{A_{ij}}{r_{ij}^{12}}-\frac{B_{ij}}{r_{ij}^{6}}\right), \tag{3}$$

$$E_{HB}=\sum_{(i,j)}\left(\frac{C_{ij}}{r_{ij}^{12}}-\frac{D_{ij}}{r_{ij}^{10}}\right), \tag{4}$$

$$E_{tor}=\sum_l U_l[1\pm\cos(n_l\chi_l)]. \tag{5}$$

Here, r_{ij} (in Å) is the distance between the atoms i and j, and χ_l is the lth torsion angle. The peptide bond angles are set to their common value $\omega=180°$. We further assume for the electrostatic permittivity in the protein interior $\varepsilon=2$ (its common value in ECEPP simulations).

Simulations of our peptide EKAYLRT in gas phase are compared with such where the interaction of the peptide with surrounding water is approximated by an implicit solvent [13]:

$$E=E_{\mathrm{ECEPP/3}}+E_{solv} \quad \text{with} \quad E_{solv}=\sum_i \sigma_iA_i. \tag{6}$$

Here, E_{solv} is the solvation energy and thought to be proportional to the solvent accessible surface area A_i of the ith atom. The parameters σ_i are experimentally determined proportionality factors.

Simulations of such detailed protein models are extremely difficult. This is because the various competing interactions lead to multitude of local energy minima separated by high barriers. Hence, in the low-temperature region, canonical Monte Carlo or molecular dynamics simulations will get trapped in one of these minima and not thermalize within the available CPU time. Only with the introduction of new and sophisticated algorithms such as *generalized-ensemble* techniques [14], is it possible to alleviate this problem in protein simulations [15]. For this reason, our investigations rely on the use of one of these techniques, multicanonical sampling [16], where conformations with energy E are assigned a weight $w_{mu}(E)\propto 1/n(E)$ [$n(E)$ is the density of states). A simulation with this weight will generate a one-dimensional random walk in the energy space and lead to a uniform distribution of energy:

$$P_{mu}(E)\propto n(E)w_{mu}(E)=\mathrm{const}. \tag{7}$$

Since a large range of energies is sampled, one can use the reweighting techniques [17] to calculate thermodynamic quantities over a wide range of temperatures T by

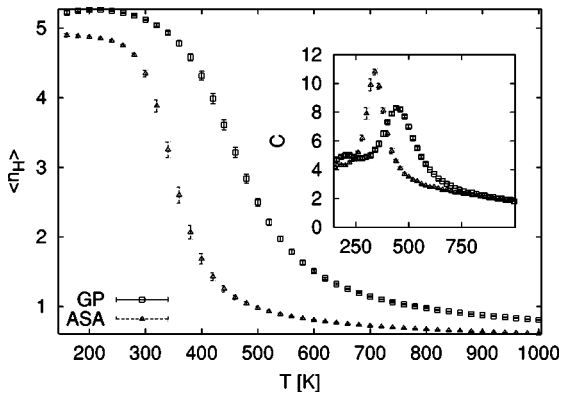

FIG. 1. The average number $\langle n_H\rangle$ of helical residues as a function of temperature T for EKAYLRT in gas phase (GP) and simulated with an implicit solvent term (ASA). The specific heat $C(T)$ as a function of temperature T is displayed in the inlet. All results rely on multicanonical simulations of 2 000 000 sweeps each.

$$\langle\mathcal{A}\rangle_T=\frac{\int dx\ \ \mathcal{A}(x)w^{-1}(E(x))\ \ e^{-\beta E(x)}}{\int dx w^{-1}(E(x))\ \ e^{-\beta E(x)}}, \tag{8}$$

where x stands for configurations and $\beta=1/k_BT$ is the inverse temperature. Estimators for the multicanonical weights $w(E)=n^{-1}(E)=\exp[-S(E)]$ can be calculated with the iterative procedures described in Ref. [6].

In our case we needed between 100 000 and 200 000 sweeps for the weight factor calculations. All thermodynamic quantities are then estimated from one production run of 2 000 000 Monte Carlo sweeps that followed 10 000 sweeps for ''thermalization.'' Our simulations start from completely random initial conformations (hot start) and one Monte Carlo sweep updates every torsion angle of the peptide once. At the end of every fourth sweep, we store the total energy E_{Tot}, the ECEPP/3 energy $E_{\mathrm{ECEPP/3}}$, its partial terms E_C, E_{LJ}, E_{HB}, and E_{tor}, the solvation energy E_{Solv}, the corresponding end-to-end distance d_{e-e}, and the number n_H (n_B) of helical (sheet) residues. Here, we follow the previous work [3] and consider a residue as helical if its backbone angles (ϕ,ψ) are within the range $(-70°\pm30°,-37°\pm30°)$. Similarly, a residue is assumed to be ''sheetlike'' if (ϕ,ψ) are within the range $(-140°\pm40°,140°\pm40°)$.

III. RESULTS AND DISCUSSION

We start with presenting our results for a single EKAYLRT molecule that is not interacting with other molecules. We display for this peptide in Fig. 1 the average helicity $\langle n_H\rangle(T)$ as a function of temperature. Data obtained in gas phase (GP) and such for simulations that rely on a solvent accessible surface area term (ASA) to approximate protein-water interactions are shown in the figure. We observe in both cases a steep helix-coil transition that separates a high-temperature region with little helicity from a low-temperature region where most of the residues are part of an α-helix. The location of this transition can be determined

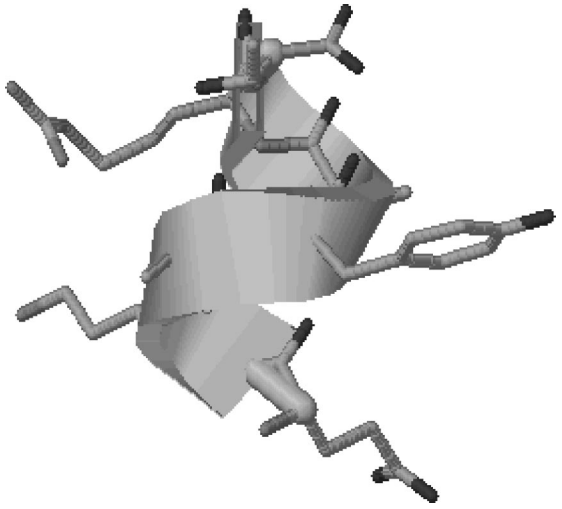

FIG. 2. Lowest-energy configuration of EKAYLRT as found in a multicanonical simulation of 2 000 000 sweeps using an implicit solvent to approximate the peptide-water interactions.

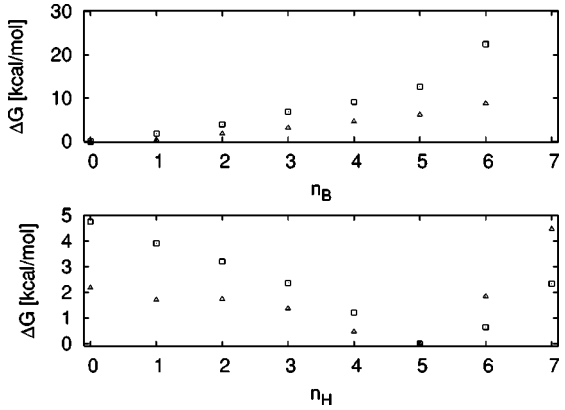

FIG. 3. The free energy ΔG at $T=300$ K as a function of (bottom) helicity n_H and (top) sheetness n_B for EKAYLRT in gas phase ($\square$) and simulated with an implicit solvent term (Δ). The free energy is normalized in such a way that its minimum value is set to zero. All results are calculated from a multicanonical simulation of 2 000 000 sweeps.

from the corresponding peaks in the specific heat $C(T)$ which are drawn in the inlet. We find the helix-coil transition temperature of EKAYLRT in gas phase as $T_{hc}^{GP}=445 \pm 15$ K. The more pronounced peak for the solvated molecule indicates a temperature $T_{hc}^{ASA}=340\pm 10$ K that is considerably lower than the one in gas phase. Unphysiologically high helix-coil transition temperatures in gas phase, and their shift toward a more sensible temperature range when an implicit solvent is introduced, have also been observed in our earlier work on homopolymers [6,7].

We show in Fig. 2, as an example for the helical configurations that dominate below T_{HC}, the lowest-energy configuration found in a simulation of the solvated peptide ($E_{Tot}=-69.6$ kcal/mol). The lowest-energy configuration in gas phase ($E_{Tot}=E_{\mathrm{ECEPP/3}}=-28.0$ kcal/mol) is also a helix (structure not shown). The energy of these helical structures is by ≈ 25 kcal/mol lower than the energy of the lowest-found sheetlike configurations: $E_{Tot}=-43.8$ kcal/mol for the solvated peptide and $E_{Tot}=E_{\mathrm{ECEPP/3}}=-3.1$ kcal/mol for EKAYLRT in gas phase.

The preference for helical structures can be also seen in Fig. 3(a) where we display the free energy ΔG at $T=300$ K as a function of helicity n_H and "sheetness" n_B. Note that for convenience we have chosen a normalization where the minimum in free energy takes a value of zero. Both in gas phase and for the solvated molecule a funnel-like free-energy landscape is formed, with the free-energy minimum at $n_H=5$, i.e., for maximal helicity (since the two terminal ends are flexible and will usually not be part of an helix, a fully formed helix has a length $n_H=5$ instead of $n_H=7$). The absolute value of the free-energy difference between coil and helix is much larger for the peptide in gas phase ($\Delta G\approx -5$ kcal/mol) than it is for the solvated molecule ($\Delta G\approx -2$ kcal/mol) indicating that the helix-coil transition is stronger for EKAYLRT in gas phase than for the molecule in an implicit solvent. This is in agreement with the earlier work where we have found similar results for polyalanine chains [7]. The corresponding projection of the free-energy landscape on the sheetness n_B in Fig. 3(b) shows the opposite picture; the free-energy increase with the number of residues whose backbone dihedral angles take values that are common in a β-sheet. Coil structures are at $T=300$ K favored over sheet-like structures by $\Delta G\approx 5$ kcal/mol in the implicit solvent and by $\Delta G\approx 8$ kcal/mol in gas phase.

The observed form of the free-energy landscape is caused solely by the intramolecular interactions. This can be seen in Fig. 4 where we plot for solvated EKAYLRT the total energy E_{Tot}, the internal energy $E_{\mathrm{ECEPP/3}}$, and the solvation energy E_{Solv} as a function of temperature. Here, we have normalized all energy terms in such a way that their value at $n_H=m0$ ($n_B=0$) is zero. Both E_{Tot} and $E_{\mathrm{ECEPP/3}}$ decrease with growing number of residues that are part of ahelix while E_{Solv} increases [Fig. 4(a)]. Hence, the protein-water interaction term opposeshelix formation. This result is rea-

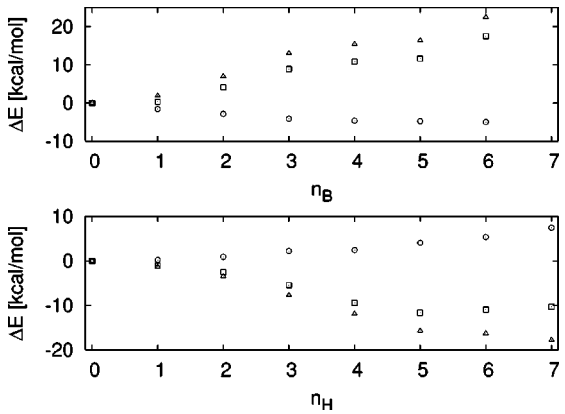

FIG. 4. The average total energy $\langle E_{Tot}\rangle$ ($\square$), intramolecular energy $\langle E_{\mathrm{ECEPP/3}}\rangle$ (Δ), and solvation energy $\langle E_{Solv}\rangle$ ($\bigcirc$) of EKAYLRT at $T=300$ K as a function of (bottom) helicity n_H and (top) sheetness n_B. All energies are normalized in such a way that their value at $n_H=0$ ($n_B=0$) is zero. All results are calculated from a multicanonical simulation of 2 000 000 sweeps using an implicit solvent model to approximate peptide-water interactions.

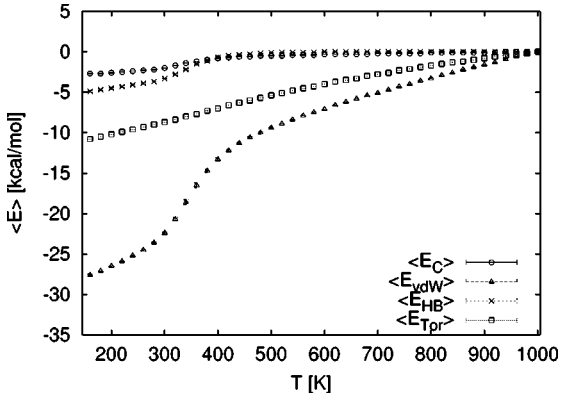

FIG. 5. The average partial energies $\langle E_C\rangle$, E_{vdW}, E_{HB}, and E_{Tor} that together make up the ECEPP/3 energy $E_{\mathrm{ECEPP/3}}$ as a function of temperature T. All terms are normalized in such a way that their value for $T=1000$ K is zero. All results are calculated from a multicanonical simulation of 2 000 000 sweeps using an implicit solvent model to approximate peptide-water interactions.

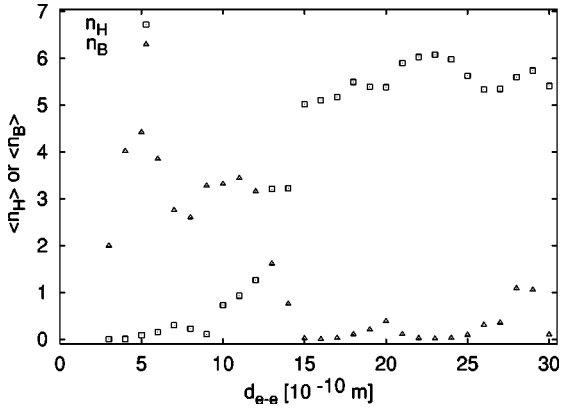

FIG. 6. The average helicity $\langle n_H\rangle$ and sheetness $\langle n_B\rangle$ at $T=300$ K of the N-terminal EKAYLRT residues as a function of the end-to-end distance $d_{e\text{-}e}$. All results are calculated from a multicanonical simulation of 2 000 000 sweeps.

sonable as the protein-water hydrogen bonds compete with the intramolecular hydrogen bonding in an α-helix and therefore weaken helix formation in solution. However, the loss in solvation energy of $\Delta\approx 4$ kcal/mol with helix formation is small when compared with the gain in $E_{\mathrm{ECEPP/3}}\approx -16$ kcal/mol, and on average, a completely formed helix ($n_H=5$) has a total energy that is by $\Delta E_{Tot}\approx -12$ kcal/mol lower than a coil configuration ($n_H=0$). Not surprisingly, we observe the opposite behavior in Fig. 4(b) where we plot the same three energies as a function of sheetness n_B. Sheetlike configurations with large numbers n_B have higher internal energy $E_{\mathrm{ECEPP/3}}$ than such with $n_B=0$ while the solvation energy E_{solv} is lower.

Hence, while at $T=300$ K the protein-water interaction seems to favorstrands and opposes helix formation, the physics of our molecule is dominated by the intramolecular energies that lead to a strong preference for α-helix formation. Fig. 5 indicates that this behavior is mainly due to the van der Waals interaction between the atoms in the peptide. In this figure, we display as a function of temperature besides the van der Waals term $\langle E_{vdW}\rangle$ also the other partial energies that together make up $E_{\mathrm{ECEPP/3}}$: the average electrostatic energy $\langle E_C\rangle$, the hydrogen-bond energy $\langle E_{HB}\rangle$, and the torsion energy $\langle E_{Tor}\rangle$.

Our results so far indicate that the peptide EKAYLRT has an intrinsic tendency to formhelices. Strands have higher free energies, of the order of $\approx$30 kcal/mol, and are rarely observed. This result is independent of whether the molecule is in gas phase or simulated with an implicit solvent. However, EKAYLRT appears *within* proteins both in helices and β-sheets. It follows that sheet formation has to be due to the interaction of the peptide with its surrounding. We conjecture that EKAYLRT forms a β-sheet if it is in the proximity of another strand. Especially, we assume that this process also happens if the peptide is close to another EKAYLRT peptide that is already in astrand configuration. Unfortunately, the present version of SMMP does not allow the simulation of two interacting proteins. Hence, in order to test our conjecture, we have studied instead the peptide NH_2-EKAYLRT-GGGG-EKAYLRT-COOH with the C-terminal EKAYLRT residues kept as β-strand. The four glycine residues form a flexible chain that holds the two EKAYLRT units together but allows their relative positions to vary. We refer to the so constructed peptide as molecule "A."

The end-to-end distance $d_{e\text{-}e}$ is a measure for the separation of the two EKAYLRT chains. Our conjecture implies that for large values of $d_{e\text{-}e}$ the N-terminal EKAYLRT assumes an α-helix while for small values of $d_{e\text{-}e}$ (i.e., close proximity to the C-terminal EKAYLRT that forms a strand) it should assume a β-sheet configuration. We have therefore calculated from the multicanonical simulation of molecule A the helicity and sheetness of the N-terminal EKAYLRT at $T=300$ K. Both quantities are displayed in Fig. 6. Two regions are observed. For $d_{e\text{-}e}>\approx 16$ Å the N-terminal EKAYLRT chain forms a complete helix andstrands are rarely observed. Hence, for these distances the N-terminal chain has a similar behavior as the isolated EKAYLRT peptide. However, for decreasing end-to-end distance, the helicity also decreases and vanishes for $d_{e\text{-}e}<\approx 10$ Å. At the same time, the sheetness increases and the peptide forms a β-sheet for $d_{e\text{-}e}\approx$5-6 Å. Note that the average potential energy of helical configurations is $\langle E_{Tot}\rangle=-24.9(1.6)$ kcal/mol within the error bars equal to that of sheetlike configurations [$\langle E_{Tot}\rangle=-23.4(2.9)$ kcal/mol].

In Fig. 7, the projection of the free-energy landscape at room temperature ($T=300$ K) on the helicity and sheetness of the N-terminal EKAYLRT residues is drawn. For convenience, we have set in this figure the lowest-found value of the free energy to zero as energies are only defined up to an additive constant. The contour lines are spaced by 2 kcal/mol. The free-energy landscape is plotted only for values of $G\leqslant 25$ kcal/mol as values of the free energy grow rapidly outside of the drawn area. We observe again two minima, corresponding to fully formed helix and β-strands. Examples of configurations that correspond to the two minima are shown in Fig. 8. Both minima have comparable free energies and are separated by barriers of only 2 kcal/mol allowing an easy interchange between the two forms.

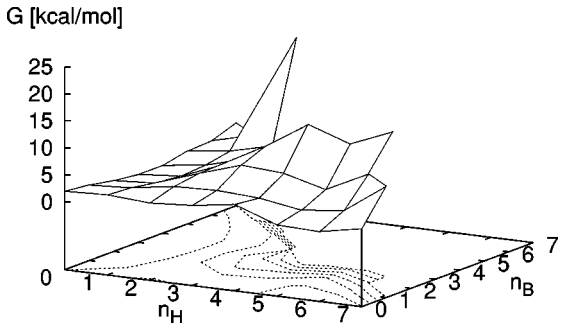

FIG. 7. The free-energy landscape of molecule *A* at room temperature ($T=300$ K) as a function of helicity $\langle n_H \rangle$ and sheetness $\langle n_B \rangle$. The global minimum is set to zero and the contour lines are spaced by 2 kcal/mol.

In order to understand in more detail why EKAYLRT forms a β-strand when close to a molecule that is already in a β-sheet form, we have performed further simulations of NH_2-EKAYLRT-GGGG-EKAYLRT-COOH holding now not only the *C*-terminal EKAYLRT residues as a β-strand but forcing also the four connecting glycine residues into a turn. We refer to the so-defined peptide as molecule "*B*." The *N*-terminal EKAYLRT residues are now by construction in close proximity to the *C*-terminal EKAYLRT strand. Hence, we expect that at room temperature the *N*-terminal EKAYLRT chain will also form a β-strand. This conjecture is supported by Fig. 9 where we plot the average sheetness n_B of the *N*-terminal EKAYLRT residues as a function of temperature. Both in gas phase and for simulations with a solvent accessible surface term, we find that on average more than five of the seven residues are part of a sheetlike structure. $\langle n_B \rangle$ decreases smoothly with growing temperature and the maximum in the specific heat is shallow. The transition is more pronounced for the peptide in an implicit solvent than for the one in gas phase, and shifted toward lower temperatures.

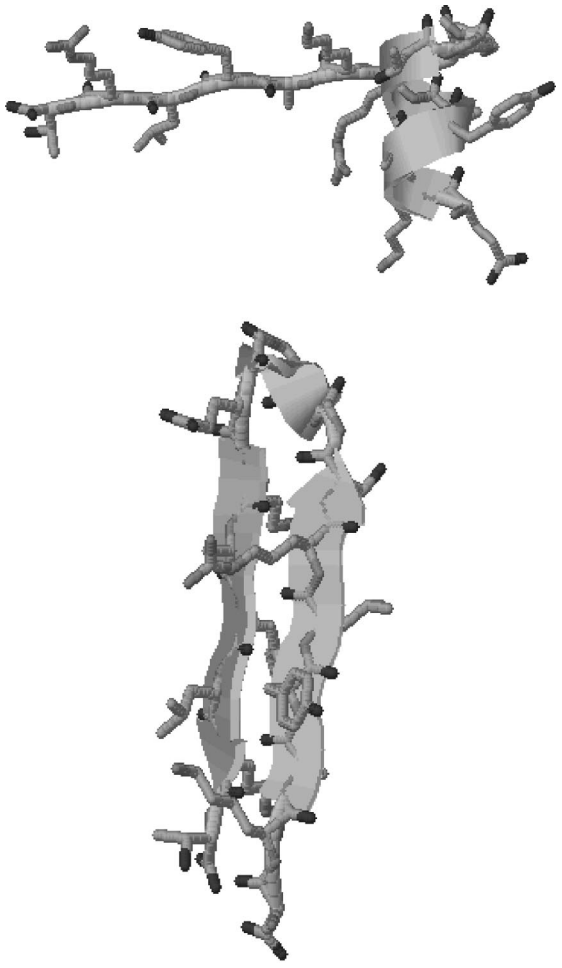

FIG. 8. Low-energy configurations of molecule *A* as found in a multicanonical simulation of 2 000 000 sweeps. The one in (a) is the lowest-energy configuration where the *N*-terminal EKAYLRT residues form an α-helix; the one in (b) where they form a β-sheet.

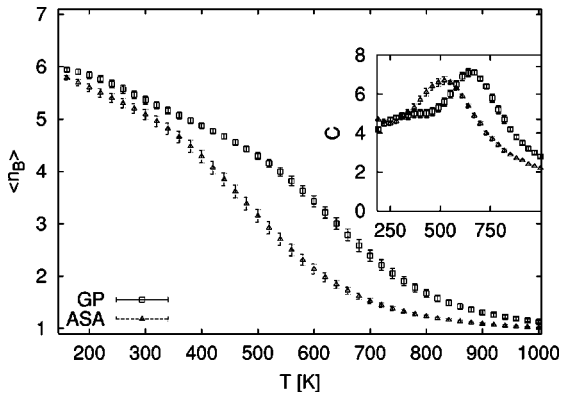

FIG. 9. The average "sheetness" $\langle n_B \rangle$ of the *N*-terminal EKAYLRT residues of molecule *B* as a function of temperature.

Unlike our previous simulations where the glycine residues could move freely, a large percentage of configurations are now at room temperature in a sheet form. The increased statistics of these configurations allows for a better analysis of the factors that help to overcome the intrinsic propensity of EKAYLRT to form an α-helix and lead to a β-sheet. Table I lists the differences of various energies between structures where the *N*-terminal EKAYLRT unit is a β-strand with structures where these residues form an α-helix. Values are listed for the whole molecule *B* and such restricted to the *N*-terminal EKAYLRT chains. Also listed are the differences of both terms. The latter quantity is a measure for the interactions between these seven residues and the rest of the molecule (which is kept fixed).

We see from this table that at $T=300$ K configurations with the *N*-terminal EKAYLRT chain in a sheet are energetically favored by 7 kcal/mol over such configurations where these residues form an α-helix. This energy bias is found for all partial energies with the exception of the solvation energy term E_{Solv} and the torsion energy term E_{Tor}. While their values seem to indicate a slight preference for helical over sheet-like configurations, they are within the error bars compatible with zero suggesting that both terms show no preference for one of the two forms.

Because of the bias in the internal energies $E^{Molecule\,B}$ of the whole molecule *B*, β-sheet-like conformations of the *N*-terminal EKAYLRT chain dominate at room temperature.

TABLE I. Energy differences between ''sheet'' and helix configurations at room temperature for various energy terms as calculated from a multicanonical simulation of molecule *B*.

	Molecule *B*	*N*-terminal EKAYLRT residues only	Background
ΔE_{Tot}	−7.2(9)	14.5(1.4)	−21.8(1.6)
ΔE_{Solv}	0.6(3)	−3.1(2)	3.7(3)
ΔE_{EL}	−4.3(3)	0.6(1)	−4.9(3)
ΔE_{vdW}	−3.2(8)	12.5(9)	−15.7(1.1)
ΔE_{HB}	−0.8(2)	4.0(2)	−4.8(3)
ΔE_{Tor}	0.5(4)	0.5(4)	0.0

However, the behavior of the various energy terms is different when one considers only the contributions by these seven residues. With the exception of the solvation energy $E_{Solv}^{EKAYLRT}$, which favors β-strands, all energy terms favor now a helix. On an average, helical structures have at $T=300$ K a 14.5(1.4) kcal/mol lower energy $E^{EKAYLRT}$ than strands when only the interaction between atoms in these seven residues is considered. Hence, their behavior is qualitatively the same as for the isolated EKAYLRT peptide where we also observed a strong bias toward helical conformations. Again, we find also that the van der Waals energy E_{vdW} is the dominant term. It follows that the β-sheet configurations that dominate when the EKAYLRT residues are build into molecule *B* are caused by the interaction between this chain and the ''background'' of the rest of the molecule. Since energies are additive, we can calculate this background field by

$$E^{Background}=E^{Molecule\ B}-E^{EKAYLRT}. \tag{9}$$

The strength of the interaction between the peptide and the background field of the rest of molecule *B* can be seen from the large energy difference of $\Delta E_{Tot}^{Background}=-21.8(1.6)$ kcal/mol by which these interactions favor a strand. The main contribution comes from the van der Waals term $[\Delta E_{vdW}^{Background}=15.7(1.1)$ kcal/mol] which is almost three times as large as the electrostatic and torsion energy terms. Note that Eq. (9) tells us also that the background given by the fixed parts of molecule *B* raises the solvation energy difference $\Delta E_{Solv}^{EKAYLRT}=-3.1(2)$ kcal/mol of the EKAYLRT chain by $\Delta E_{Solv}^{Background}=3.7(3)$ kcal/mol to a value of $\Delta E_{Solv}^{Molecule\ B}=0.6(3)$ kcal/mol for the whole system. This is because the term $\Delta E_{Solv}^{EKAYLRT}$ is due to the competition between hydrogen-bond formation in an α-helix and hydrogen-bond formation between the peptide and the surrounding water. However, in molecule *B* the peptide is geometrically constraint in such a way that this competition is replaced by one between hydrogen-bond formation in an α-helix of the *N*-terminal EKAYLRT on one side, and formations of hydrogen bonds between the peptide and the *C*-terminal EKAYLRT residues on the other side (see also the opposite sign of the terms $\Delta E_{HB}^{EKAYLRT}$ and $\Delta E_{HB}^{Background}$ in Table I). As a result, both the solvation energy difference $\Delta E_{Solv}^{Molecule\ B}$ and hydrogen-bond energy difference $\Delta E_{HB}^{Molecule\ B}$ are marginal. Instead, the preference of β-sheet configurations for EKAYLRT in the background of the fixed rest of molecule *B* seems to be mainly due to the electrostatic and van der Waals energies. This is reasonable: a β-sheet conformation allows for an average closer distance between the atoms of the *N*-terminal EKAYLRT chain and the existing β-strand of the *C*-terminal EKAYLRT residues, decreasing in this way the van der Waals energy. At the same time, the alignment of the two β-strands leads also to a favorable alignment of the dipole moments associated with each residue lowering therefore the electrostatic energy. We conjecture that without the stereometric constraints imposed by the connecting glycine residues the two strands would move together and aggregate as the energy gain increases with decreasing distance between them.

Our above presented results for molecule *A* and molecule *B* suggest autocatalytic properties for EKAYLRT: if the peptide forms a strand, it becomes energetically favorable for other nearby EKAYLRT molecules to transform themselves into a sheet (instead of the normally preferred helix), and eventually to aggregate with the first one. This behavior is similar to the mechanism thought to be responsible for the outbreak of neurodegenerative illnesses such as Alzheimer's or the prion diseases. Outbreak of theses illnesses is associated with the appearance of a misfolded structure that differs from the correctly folded one by a β-sheet instead of an α-helix. The misfolded structure is thought to be autocatalytic, that is, its presence leads to a structural transition by which the correctly folded (helical) structure changes into the harmful β-sheet form. Hence, peptides that contain the sequence of amino acids EKAYLRT can serve as simple models to study these $\alpha\rightarrow\beta$ transitions and the mechanism of prion diseases. For instance, our investigation suggests that the formation of β-sheets can be minimized by shielding the surface area of already existing β-sheet forms, minimizing in this way the van der Waals interaction. Another possibility may be to introduce metal ions that alter the electrostatic interaction decreasing in this way the energy bias toward β-sheets.

IV. CONCLUSION

We have performed multicanonical simulations of peptides that contain the sequence of amino acids EKAYLRT. We find that the EKAYLRT-peptide itself has both in gas phase and in solution an intrinsic tendency to form an α-

helix. However, the peptide assumes a β-sheet form when close to another strand. The transition from an α-helix toward a β-sheet is caused by strong van der Waals and electrostatic energy terms that favor the β-sheet form when EKAYLRT is in close proximity to another strand. This autocatalytic property of EKAYLRT, which induces strand formation in other EKAYLRT molecules when in a β-sheet configuration, suggests that the EKAYLRT based peptides can serve as a simple model for the $\alpha \rightarrow \beta$ transitions and successive aggregation that are supposed to be related to the outbreak of various illnesses such as Alzheimer's or the prion diseases.

ACKNOWLEDGMENTS

U.H. gratefully acknowledges support through a research grant from the National Science Foundation (Grant No. CHE-9981874). Part of this paper was written while U.H. visited the University of Central Florida in Orlando, FL. He acknowledges the UCF Physics Department for kind hospitality.

[1] S. Sudarsanam, Proteins **30**, 228 (1998).
[2] D.L. Minor, Jr. and P.S. Kim, Nature (London) **380**, 730 (1996).
[3] Y. Okamoto and U.H.E. Hansmann, J. Phys. Chem. **99**, 11 276 (1995).
[4] U.H.E. Hansmann and Y. Okamoto, J. Chem. Phys. **110**, 1267 (1999); **111**, 1339(E) (1999).
[5] N.A. Alves and U.H.E. Hansmann, Phys. Rev. Lett. **84**, 1836 (2000).
[6] Y. Peng and U.H.E. Hansmann, Biophys. J. **82**, 3269 (2002).
[7] Y. Peng, U.H.E. Hansmann, and N.A. Alves, J. Chem. Phys. **118**, 2374 (2003).
[8] N.A. Alves and U.H.E. Hansmann, J. Chem. Phys. **117**, 2337 (2002).
[9] A. Wind, J.P. Kemp, A. Ermoshkin, and J.Z.Y. Chen, Phys. Rev. E **66**, 031909 (2002).
[10] J.Z.Y. Chen, A.S. Lemak, J.R. Lepock, and J.P. Kemp, Proteins: Struct., Funct., Genet. **51**, 283 (2003).
[11] G. Némethy, K.D. Gibson, K.A. Palmer, C.-N. Yoon, G. Paterlini, A. Zagari, S. Rumsey, and H.A. Scheraga, J. Phys. Chem. **96**, 6472 (1992).
[12] F. Eisenmenger, U.H.E. Hansmann, Sh. Hayryan, and C.-K. Hu, Comput. Phys. Commun. **138**, 192 (2001).
[13] T. Ooi, M. Obatake, G. Nemethy, and H.A. Scheraga, Proc. Natl. Acad. Sci. U.S.A. **8**, 3086 (1987).
[14] U.H.E. Hansmann and Y. Okamoto, in *Annual Reviews in Computational Physics VI*, edited by D. Stauffer (World Scientific, Singapore, 1998), p. 129.
[15] U.H.E. Hansmann and Y. Okamoto, J. Comput. Chem. **14**, 1333 (1993).
[16] B.A. Berg and T. Neuhaus, Phys. Lett. B **267**, 249 (1991).
[17] A.M. Ferrenberg and R.H. Swendsen, Phys. Rev. Lett. **61**, 2635 (1988); **63**, 1658(E) (1989), and references given in the erratum.